Coupling of Crossed Planar Multiconductor Systems

WERNER VEIT, HEINRICH DIESTEL, AND REINHOLD PREGLA, SENIOR MEMBER, IEEE

Abstract—**Capacitive couplings between orthogonally crossed, galvanically separated transmission lines are analyzed using the "method of lines." The static capacitances of typical stripline configurations are calculated. Charge density distributions occurring when two parallel striplines are crossed by a third are described.**

I. Introduction

IN DIGITAL integrated circuits, interconnection lines on different dielectric layers frequently cross orthogonally. Couplings between these galvanically separated transmission lines are therefore predominantly capacitive. In MMIC's such stripline crossings are used as air bridges or underpasses, e.g. for spiral inductors and directional couplers.

Although multiconductor crossings occur in many circuits, little has been reported on the characteristics of such complex structures. A static spectral-domain approach is used in [1] for calculating the coupling capacitances of air bridges and underpasses. A full-wave analysis for determining the equivalent circuit parameters of a single, stripline crossing is shown in [2]. However, this method, which is based on the generalized "transverse resonance technique," is rather cumbersome for configurations with more than four ports. In many cases simple parallel-plate estimations of the coupling capacitances are used for CAD purposes. Because of the large extent of the coupling field, such models cannot provide sufficiently accurate network parameters.

This paper describes a field-theory-based method of calculating the lumped capacitances of crossed planar multiconductor systems. An equivalent circuit representation is derived for a single stripline crossing, and the static capacitances are compared with the corresponding capacitances given in [2] at the frequency $f = 2.0$ GHz. Charge density distributions are presented for an underpass, consisting of two strips crossed orthogonally by a third one. Finally, a capacitance matrix for an arrangement of three coupled stripline crossings is given.

Manuscript received June 15, 1989; revised September 28, 1989.

W. Veit is with Siemens AG, Balanstr. 73, D-8000 Munich 80, West Germany.

H. Diestel is with Siemens AG, Hofmannstr. 51, D-8000 Munich 70, West Germany.

R. Pregla is with the FernUniversität Hagen, Allgemeine and Theoretische Elektrotechnik, Postfach 940, D-5400 Hagen, West Germany.

IEEE Log Number 8932997.

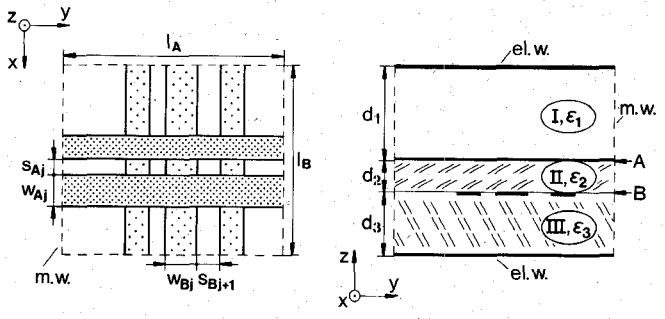

Fig. 1. Top and cross-sectional views of two orthogonally crossed planar multiconductor systems at different dielectric interfaces; d_k and ϵ_k denote the thickness and the permittivity of the kth layer; the width of the jth stripline at interface A (B) and the width of the spacing that follows are given by $w_{A(B)j}$ and $s_{A(B)j+1}$, respectively; $l_{A(B)}$ is the length of the striplines at interface A (B). The structure is bounded by magnetic and electric walls (m./el.w.).

II. Analysis

We consider the potential function $\varphi(x, y, z)$, which must satisfy Laplace's differential equation $\Delta\varphi = 0$ in the different regions (I) to (III) of Fig. 1. Dirichlet's and Neumann's conditions hold at the electric and magnetic walls. For solving this boundary value problem using the method of lines, the differential quotients with respect to x and y in Laplace's differential equation are replaced by finite difference expressions.

A typical pattern for discretization of a stripline crossing is illustrated in Fig. 2. The lines of discretization run parallel to the z axis and are marked by "+" and "•" in the $x-y$ plane. The potential function $\varphi(x_i, y_k, z) = \varphi_{i,k}$ and the second derivatives $\varphi_{xx}(x_i, y_k, z)$ and $\varphi_{yy}(x_i, y_k, z)$ are evaluated at the line (x_i, y_k, z), marked by "+" in the detail. The first derivatives are related to locations between the potential lines; i.e., $\varphi_x(y_k, z)|_i$ is evaluated at (a) and $\varphi_y(x_i, z)|_k$ is determined at location (b). The mixed derivative $\varphi_{xy}(z)|_{i,k}$ is calculated at one of the corners of the rectangular mesh of the area $e_{xi} \times e_{yk}$. If we assign this mesh to its central line, where $\varphi_{i,k}$ is evaluated, the following simple geometrical interpretation holds: each line (i, k), marked by "+," has its "own" mesh of area $e_{xi} \times e_{yk}$. The corners of these meshes, marked by "•," represent the central lines of another, shifted net with meshes of area $h_{xi} \times h_{yk}$.

In the present method of analysis the potential function is discretized with respect to x and y; i.e., the differential

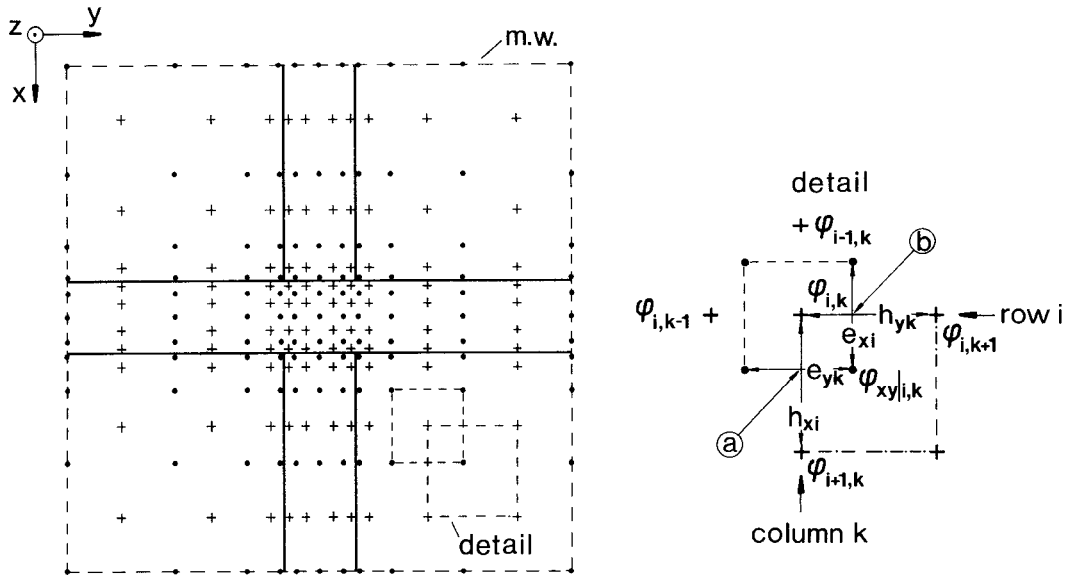

Fig. 2. Top view of a stripline crossing. The lines of discretization for the potential function and the second derivatives are marked in the $x-y$ plane by "+." The first derivatives $\varphi_x|_l$ and $\varphi_y|_k$ are evaluated at the locations ⓐ and ⓑ, as is indicated in the detail. The mixed first derivative $\varphi_{xy}|_{l,k}$ is calculated at the corner of the mesh of area $e_{xl} \times e_{yk}$; h_{xl} and h_{yk} denote the widths of the shifted mesh.

quotients for these variables are approximated by finite difference expressions [3]. If we define the first-order operator with respect to x by $[\bar{D}_x] = [r_{hx}][D_x][r_{ex}]$, where $[D_x]$ denotes a bidiagonal difference operator [4], the following approximate relation for the matrix of the $Mx \times My$ second derivatives holds:

$$\begin{aligned} h^2[r_{ex}]^{-1}[\varphi_{xx}][r_{ey}]^{-1} &= h^2[\Phi_{xx}] \\ &= -[\bar{D}_x]^t[\bar{D}_x][\Phi] \\ &= [\bar{D}_{xx}][\Phi]. \end{aligned} \tag{1}$$

The elements of the matrix $[\Phi]$ represent the normalized potentials $[\Phi]_{l,k} = [\varphi]_{l,k}/(\sqrt{h/e_{xl}}\sqrt{h/e_{yk}})$.

In accordance with [3], the intermediate transformation, called normalization, is performed by diagonal matrices. In the special case of equidistant discretization, the four matrices of different order $[r_{ex(ey)}] = \mathrm{diag}(\sqrt{h/e_{xi(yk)}})$ and $[r_{hx(hy)}] = \mathrm{diag}(\sqrt{h/h_{xi(yk)}})$, which depend on the mesh widths e_{xl}, e_{yk} and h_{xl}, h_{yk}, equal the corresponding unity matrices.

A finite difference approximation similar to (1) can be given for the second derivatives with respect to y. However, for the position of $[\varphi]_{l,k}$ in matrix $[\varphi]$ to equal the position of the corresponding marking "+" in the discretization pattern, we must interchange the matrices of potential and operator $[\bar{D}_{yy}]$. Laplace's differential equation is solved at the $Mx \times My$ nodes of the net marked by "+." For the normalized potential the following approximate equation holds:

$$\frac{d^2}{dz^2}[\Phi] + \frac{1}{h^2}[\bar{D}_{xx}][\Phi] + [\Phi][\bar{D}_{yy}]\frac{1}{h^2} = [0] \tag{2}$$

with the real, symmetric, and tridiagonal second-order operators $[\bar{D}_{xx}]$ and $[\bar{D}_{yy}]$.

A twofold discretized function is represented clearly by a two-dimensional matrix. For the mathematical and computational solution of the boundary value problem, however, the representation of the discrete potential function in the form of a vector is more advantageous [5]. Hence, instead of (2), the following equivalent equation is solved:

$$\frac{d^2}{dz^2}\vec{\Phi} + \frac{1}{h^2}\left[\hat{\bar{D}}_{xx}\right]\vec{\Phi} + \frac{1}{h^2}\left[\hat{\bar{D}}_{yy}\right]\vec{\Phi} = \vec{0} \tag{3}$$

with the vector $\vec{\Phi} = (\vec{\Phi}_1, \cdots, \vec{\Phi}_{My})^t$, whose elements are the column vectors of the matrix $[\Phi]$.

The second-order operators take the form of block matrices, defined by $[\hat{\bar{D}}_{xx}] = [I]_{My} \otimes [\bar{D}_{xx}]$ and $[\hat{\bar{D}}_{yy}] = [\bar{D}_{yy}] \otimes [I]_{Mx}$, where $[I]_{My(Mx)}$ denotes the unit matrix of order $My(Mx)$ and the symbol "$\otimes$" designates a Kronecker product (see the Appendix, eq. (A1)).

The potentials $[\Phi]_{l,k}$ of (2) are coupled. Decoupling is achieved by a real transformation of the operators $[\bar{D}_{xx}]$ and $[\bar{D}_{yy}]$, respectively [3], [4]. By this the operators of (3) are transformed to the block diagonal structure of their eigenvalues; i.e., $[\hat{T}]^t[\hat{\bar{D}}_{xx(yy)}][\hat{T}] = -[\hat{\chi}_{x(y)}]^2$, with the matrix of eigenvectors $[\hat{T}] = [T_y] \otimes [T_x]$, where $[T_x]$ and $[T_y]$ are the eigenvector matrices for the operators of (2).

The transformation of (3) yields the following set of $MxMy$ ordinary differential equations:

$$\frac{d^2}{dz^2}\tilde{\vec{\Phi}} - [\hat{\chi}_z/h]^2\tilde{\vec{\Phi}} = \tilde{\vec{0}} \tag{4}$$

where $\tilde{\vec{\Phi}} = [\hat{T}]^t\vec{\Phi}(z)$. The relation $[\hat{\chi}_z/h]^2 = [\hat{\chi}_x/h]^2 + [\hat{\chi}_y/h]^2$, which corresponds to the separation equations, as given with Fourier series expansions, holds for the eigenvalues. Matching of the fields at the interfaces $z = d_2$

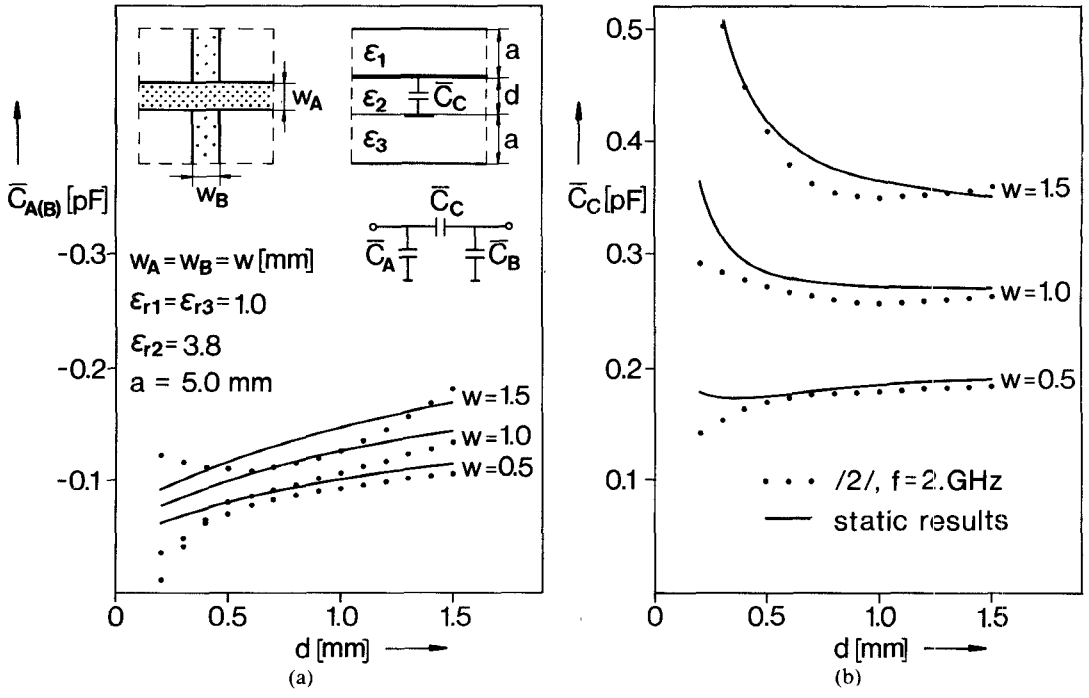

Fig. 3. Equivalent circuit capacitances $\bar{C}_A$, $\bar{C}_B$ ($=\bar{C}_A$), and $\bar{C}_C$ versus substrate thickness d for a crossing of two striplines.

(A) and $z = 0$ (B) results in the equation

$$\begin{bmatrix} \tilde{\vec{\Phi}}_A \\ \tilde{\vec{\Phi}}_B \end{bmatrix} = \begin{bmatrix} [\tilde{\Gamma}_{11}] & [\tilde{\Gamma}_{12}] \\ [\tilde{\Gamma}_{21}] & [\tilde{\Gamma}_{22}] \end{bmatrix} \begin{bmatrix} \tilde{\vec{Q}}_A \\ \tilde{\vec{Q}}_B \end{bmatrix} \tag{5}$$

where the $[\tilde{\Gamma}_{nm}]$ are block diagonal matrices of order $MxMy$. The transformed potentials and charges are related to the corresponding vectors in the original domain by $\vec{\varphi}_{A(B)} = [\hat{r}_e][\hat{T}]\tilde{\vec{\Phi}}_{A(B)}$ and $\vec{q}_{A(B)} = [\hat{r}_e]^{-1}[\hat{T}]\tilde{\vec{Q}}_{A(B)}$, with $[\hat{r}_e] = [r_{ey}] \otimes [r_{ex}]$. After inverse transformation of (5) into the original domain and after inversion of the reduced matrix, one obtains the equation

$$\vec{q}_{\text{red}} = [\gamma]_{\text{red}}^{-1}\vec{\varphi}_{\text{red}} = [c]\vec{\varphi}_{\text{red}}. \tag{6}$$

The $[c]_{l,k}$ represent microcapacitances. The macro- or conductor capacitances are calculated by partitioning $[c]$ and summing the appropriate terms. This yields

$$\vec{q}_{\text{cond}} = [C_{\text{cond}}]\vec{u} \tag{7}$$

with the vector of the charges of the N conducting strips $\vec{q}_{\text{cond}} = (q^{①}, \cdots, q^{Ⓝ})^t$ and the corresponding potentials $\vec{u} = (\varphi^{①}, \cdots, \varphi^{Ⓝ})^t$. The elements of the matrix $[C_{\text{cond}}]$ denote total capacitances.

III. Computation

In some analytical methods special basis functions are introduced to take account of the singular behavior of the field at the stripline edges [1], [2]. The present method uses a different approach to increase the rate of convergence and thus to save computation time. Since the mesh widths, given by the four diagonal matrices $[r_{ex}]$, $[r_{ey}]$ and $[r_{hx}]$, $[r_{hy}]$ are variable, they are chosen according to the variation of the field function.

A first approximation for an optimal discretization of the charge density distributions on the strips and the electric field at the interfaces between the strips is given in [3]. In the outer regions, bounded by the magnetic walls, the potential function varies slowly. A sufficiently large shift of the walls is achieved with small computational effort if the quotients of successive mesh widths $h_{xi(yk)}$ are fixed at 2.0.

In order to obtain a coupling model in the form of a lumped-element equivalent circuit, the capacitance matrix of the multiconductor system of length l_A (l_B) at interface A (B) (cf. Fig. 1) is calculated in the absence of the striplines at interface B (A). These two matrices represent the submatrices of the block diagonal capacitance matrix $[C_{\text{mult}}]$, which consequently does not take account of the coupling between the two crossed multiconductor systems. The lumped capacitances $[\bar{C}_{\text{eq}}]_{l,k}$ of the equivalent circuit are derived from the capacitance matrix $[C_{\text{eq}}] = [C_{\text{cond}}] - [C_{\text{mult}}]$, where $[C_{\text{cond}}]$ (cf. eq. (7)) implies the coupling of all striplines. The matrix of the lumped capacitances $[\bar{C}_{\text{eq}}]$ is defined by $[\bar{C}_{\text{eq}}]_{l,k} = -[C_{\text{eq}}]_{l,k}$, if $i \neq k$, and $[\bar{C}_{\text{eq}}]_{l,l} = \Sigma_k [C_{\text{eq}}]_{l,k}$.

In the following the bar refers to lumped capacitances for equivalent circuits.

IV. Results

The crossing of two striplines located at the different interfaces A and B is characterized by the equivalent circuit sketched in Fig. 3(a). The diagram represents the lumped capacitances $\bar{C}_A$ and $\bar{C}_B$ ($=\bar{C}_A$) as a function of the substrate thickness d for different strip widths w. The

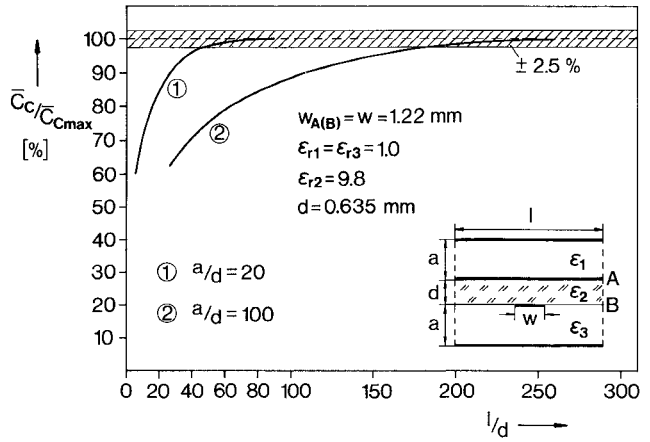

Fig. 4. Coupling capacitance $\bar{C}_C$, normalized to the final value $\bar{C}_{C\max}$, versus $1/d$ for different values of a/d.

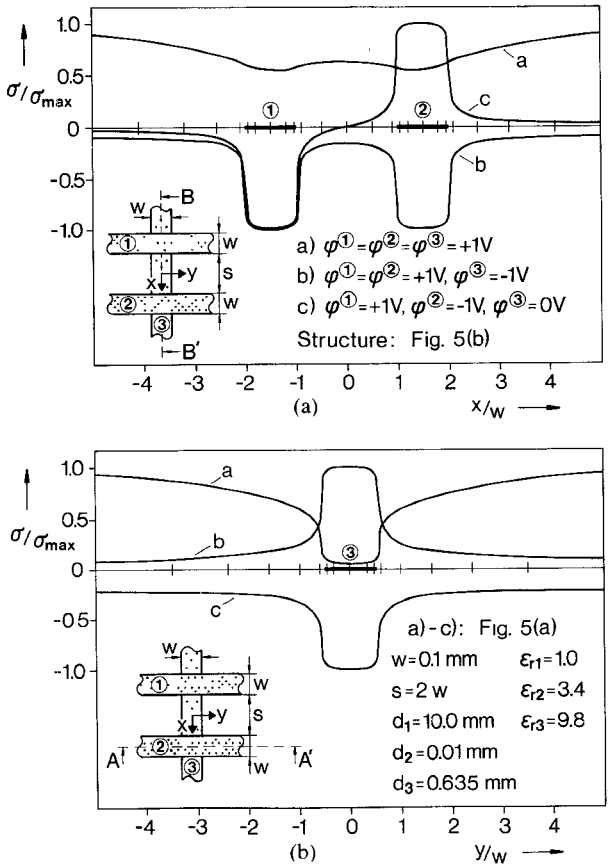

Fig. 5. Normalized charge density distributions of the planar multiconductor system sketched in the figure. For the three different cases of stripline potentials a)–c), Fig. 5(a) shows the distributions at the cut $B-B'$ and Fig. 5(b) gives the charge densities at the cut $A-A'$ for the same structure.

values of capacitance from the transverse resonance analysis of [2] at the frequency $f = 2.0$ GHz are drawn in for comparison. Fig. 3(b) shows the coupling capacitance $\bar{C}_C$ of the crossing, defined in Fig. 3(a). As is seen, at low frequencies the static equivalent capacitances provide a fairly accurate description of the stripline coupling.

The static coupling field of unshielded stripline crossings extends infinitely. In real circuits, however, we have physical boundaries, so that the electric energy is confined to a finite region. For a crossing of two striplines the convergence of the coupling capacitance $\bar{C}_C$ is examined in Fig. 4. $\bar{C}_C/\bar{C}_{C\max}$ is represented as a function of the normalized magnetic wall distance $1/d$ for two different electric wall distances a, normalized to the substrate thickness d. As is seen, in both cases of a/d the convergence of the function $\bar{C}_C$ to the final value $\bar{C}_{C\max}$ is monotonic. With an increase in a/d, we must increase $1/d$ to achieve the given range of accuracy. The final value of $a/d = 20$ is given by $\bar{C}_{C\max} = 0.959$ pF. In the case of $a/d = 100$, a reduced matrix of order 200 has been inverted to obtain the final value $\bar{C}_{C\max} = 1.506$ pF.

For calculating the lumped capacitances, four lines of discretization for the strips in the transverse direction have been chosen. Doubling this number changes the capacitance $\bar{C}_C$ by less than 0.5 percent.

In Fig. 5, surface charge density distributions at two cuts are depicted for an underpass consisting of two parallel striplines crossed orthogonally by a third one. Fig. 5(a) shows the normalized surface charge density at the midline of the single strip at interface B (cut $B-B'$) for three cases of stripline potentials: a) $\varphi^{①} = \varphi^{②} = \varphi^{③} = +1$ V; b) $\varphi^{①} = \varphi^{②} = +1$ V, $\varphi^{③} = -1$ V; c) $\varphi^{①} = +1$ V, $\varphi^{②} = -1$ V, $\varphi^{③} = 0$ V. The markings on the abscissa refer to the lines of discretization. In Fig. 5(b) the surface charge densities at the midline of conductor ② at interface A (cut $A-A'$) for the three cases of potential a)–c) are plotted. The charge density distributions of Fig. 5 are quite similar to those given in [1], except within the crossing regions. As a consequence of the singular basis functions, the charge density distributions of [1] exhibit depressions, which do not exist physically.

For an arrangement of three parallel strips at interface B crossed by a single conductor, the matrix of the lumped capacitances $[\bar{C}_{eq}]$ has been calculated. The structure is defined by $\epsilon_{r1} = \epsilon_{r2} = 1.0$, $\epsilon_{r3} = 9.8$ and has the dimensions (mm) $d_1 = 15.0$, $d_2 = 0.05$, $d_3 = 0.635$, $w_{B1} = 0.15$, $s_{B2} = 0.1$, $w_{B2} = 0.25$, $s_{B3} = 0.15$, $w_{B3} = 0.2$, and $w_{A1} = 0.15$. We obtain the capacitance matrix (fF)

$$[\bar{C}_{eq}] = \begin{bmatrix} -48.30 & 19.04 & 19.77 & 23.0 \\ 19.04 & -7.28 & -2.54 & -0.59 \\ 19.77 & -2.54 & -4.04 & -2.59 \\ 23.0 & -0.59 & -2.59 & -8.26 \end{bmatrix}.$$

As is given with the single crossing (Fig. 3), the coupling capacitances for striplines of different interfaces are positive.

V. Conclusions

A method for the static analysis of crossed planar multiconductor systems is presented. It is shown that for low frequencies the static equivalent circuit describes the stripline crossing fairly accurately. The capacitance matrix and different charge density distributions are given for stripline arrangements consisting of three and two crossings, respectively.

APPENDIX

Let $[A]$ and $[B]$ be $m \times n$ and $p \times q$ respectively. Then the Kronecker product is that $mp \times nq$ matrix defined by

$$[A] \otimes [B] = \begin{bmatrix} a_{11}[B] & \cdots & a_{1n}[B] \\ \vdots & & \vdots \\ a_{m1}[B] & \cdots & a_{mn}[B] \end{bmatrix}. \quad \text{(A1)}$$

REFERENCES

[1] L. Wiemer and R. H. Jansen, "Determination of coupling capacitance of underpasses, air bridges and crossings in MICs and MMICs," *Electron. Lett.*, vol. 23, no. 7, pp. 344–346, 1987.

[2] T. Uwano, R. Sorrentino, and T. Itoh, "Characterization of strip line crossing by transverse resonance analysis," *IEEE Trans. Microwave Theory Tech.*, vol. MTT-35, pp. 1369–1376, Dec. 1987.

[3] H. Diestel, "Analysis of planar multiconductor transmission-line systems with the method of lines," *Arch. Elek. Übertragung.*, vol. 41, no. 3, pp. 169–175, 1987.

[4] S. B. Worm and R. Pregla, "Hybrid-mode analysis of arbitrarily shaped planar microwave structures by the method of lines," *IEEE Trans. Microwave Theory Tech.*, vol. MTT-32, pp. 191–196, Feb. 1984.

[5] R. Pregla and W. Pascher, "The method of lines," in *Numerical Techniques for Microwave and Millimeter-Wave Passive Structures*, T. Itoh, Ed. New York: Wiley, 1988.

✠

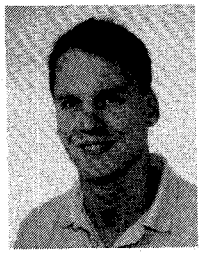

Werner Veit was born in Munich, West Germany, in 1960. He received the Dipl.-Ing. (FH) degree in technical physics from the Fachhochschule of Munich in 1986 and the Dipl.-Ing. degree in electrical engineering from the FernUniversität of Hagen, West Germany, in 1988.

Since 1988 he has been with the Siemens Components Group, Munich, where he is engaged in the design of analog CMOS integrated circuits for telecommunications.

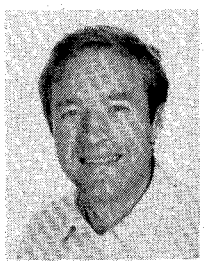

Heinrich Diestel was born in 1952. He received the Dipl.-Ing. degree from the Technical University of Hannover, West Germany, in 1978 and the Dr.-Ing. degree from the FernUniversität of Hagen, West Germany, in 1984.

Since 1984 he has been with Siemens AG, Munich, where he was engaged in the computer aided design of microwave and millimeter-wave integrated circuits. He is currently working on switching networks.

✠

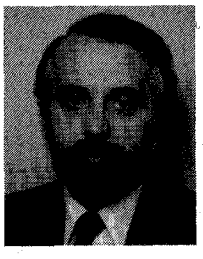

Reinhold Pregla (M'76–SM'83) was born in Luisenthal on August 5, 1938. He received the master's degree in electrical engineering (Dipl.-Ing.) and his doctorate of engineering (Dr.-Ing.) from the Technische Universität Braunschweig, West Germany, in 1963 and 1966, respectively.

From 1966 to 1969,he was a Research Assistant in the Department of Electrical Engineering of the Technische Universität Braunschweig (Institut für Hochfrequenztechnik), where he was engaged in investigations of microwave filters. After the Habilitation, he was a Lecturer in high frequencies at the Technische Universität Bochum, West Germany. Since 1975, he has held a position as full Professor in electrical engineering at the FernUniversität (a university for distance study) in Hagen, West Germany. His fields of investigation include microwave filters, waveguide theory, and antennas.